

REPORT DOCUMENTATION PAGE

Form Approved
OMB No. 0704-0188

Public reporting burden for this collection of information is estimated to average 1 hour per response, including the time for reviewing instructions, searching existing data sources, gathering and maintaining the data needed, and completing and reviewing this collection of information. Send comments regarding this burden estimate or any other aspect of this collection of information, including suggestions for reducing this burden to Department of Defense, Washington Headquarters Services, Directorate for Information Operations and Reports (0704-0188), 1215 Jefferson Davis Highway, Suite 1204, Arlington, VA 22202-4302. Respondents should be aware that notwithstanding any other provision of law, no person shall be subject to any penalty for failing to comply with a collection of information if it does not display a currently valid OMB control number. **PLEASE DO NOT RETURN YOUR FORM TO THE ABOVE ADDRESS.**

1. REPORT DATE (DD-MM-YYYY) 25-07-2000		2. REPORT TYPE Final Report		3. DATES COVERED (From - To) 01-09-1996 to 31-03-1999	
4. TITLE AND SUBTITLE Elevated Temperature Process Zone Modeling of Small Cracks in Structural Ceramics under Static and Cyclic Loading				5a. CONTRACT NUMBER	
				5b. GRANT NUMBER F49620-96-1-0451	
				5c. PROGRAM ELEMENT NUMBER	
6. AUTHOR(S) Prof. Kenneth W. White, Dept. of Mechanical Engineering, Univ. Of Houston Prof. Albert S. Kobayashi, Dept. of Mechanical Engineering, Univ. of Washington				5d. PROJECT NUMBER	
				5e. TASK NUMBER	
				5f. WORK UNIT NUMBER	
7. PERFORMING ORGANIZATION NAME(S) AND ADDRESS(ES) Dept. of Mechanical Engineering University of Houston Houston, TX 77204-4792				8. PERFORMING ORGANIZATION REPORT NUMBER Dept. of Mechanical Engineering University of Washington Seattle, Washington 98195	
9. SPONSORING / MONITORING AGENCY NAME(S) AND ADDRESS(ES) AFOSR/NA 801 N. Randolph St. Suite 732 Arlington, VA 22203-4792				10. SPONSOR/MONITOR'S ACRONYM(S) AFOSR	
				11. SPONSOR/MONITOR'S REPORT NUMBER(S)	
12. DISTRIBUTION / AVAILABILITY STATEMENT Approved for public release; distribution unlimited.					
13. SUPPLEMENTARY NOTES					
14. ABSTRACT This project focused on the study of the effects of microstructural features on the fracture process of high temperature structural ceramic materials that operate under cyclic loading environments. The ability to model these effects and the prediction of the deformation behavior also become an important consideration, as it provides a direct link to the design cycle for both, processing and design engineers. The project evaluated cyclic effects, high cycle fatigue behavior, and elevated temperature effects under these conditions. Evaluation of the effects of cyclic loading are performed using pre-cracked tensile test specimens (PFT) and bulk specimens by Moiré Interferometry. Development of finite element and simple micromechanical models for predictions of the observed behavior also presented. It is observed that hysteretic load-displacement loops arise as the primary characteristic of the behavior, although gross-slip behavior is seen under certain circumstances.					
15. SUBJECT TERMS fracture resistance; elevated temperature; structural ceramics					
16. SECURITY CLASSIFICATION OF: unclassified			17. LIMITATION OF ABSTRACT UL	18. NUMBER OF PAGES 19	19a. NAME OF RESPONSIBLE PERSON
a. REPORT	b. ABSTRACT	c. THIS PAGE			19b. TELEPHONE NUMBER (include area code)

Standard Form 298 (Rev. 8-98)
Prescribed by ANSI Std. Z39.18

20001208 035

DTIC QUALITY INSPECTED 4

UNIVERSITY OF HOUSTON

Department of Mechanical Engineering

Houston, TX 77204-4792

Phone: (713) 743-4526

Fax: (713) 743-4527

E-mail: kwwwhite@uh.edu

FINAL REPORT

SUBMITTED TO Air Force Office of Scientific Research

Bolling AFB, DC 20332-6448

Title: **Fracture Process Zone Modeling of Small Cracks in Structural Ceramics
under Static and Cyclic Loading**

May 2000

AFOSR Grant: F49620-96-1-0451

Institution Name: University of Houston
Department of Mechanical Engineering
Houston, TX 77204-4792

Principal Investigator: Kenneth W. White
Dept. of Mechanical Engineering N233D
(713) 743-4526

Co-Principal Investigator: Albert S. Kobayashi
Dept. of Mechanical Engineering FU-10
(206) 543-5488

Business Office: Thomas Lee Boozer, Director
Office of Contracts and Grants
Houston, TX 77204-2163
(713) 743-9240

Type of Organization: Educational

FRACTURE PROCESS ZONE MODELING OF SMALL CRACKS IN STRUCTURAL CERAMICS UNDER STATIC AND CYCLIC LOADING

AFOSR Grant: F49620-96-1-0451

Final Report, May 2000

Principal Investigator: Kenneth W. White
Dept. of Mechanical Engineering N233 D
Houston, TX 77204-4792

Co-Principal Investigator: Albert S. Kobayashi
Dept. of Mechanical Engineering FU-10
University of Washington

Abstract

This project focused on the study of the effects of microstructural features on the fracture process of high temperature structural ceramic materials that operate under cyclic loading environments. The ability to model these effects and the prediction of the deformation behavior also become an important consideration, as it provides a direct link to the design cycle for both, processing and design engineers.

The project evaluated cyclic effects, high cycle fatigue behavior, and elevated temperature effects under these conditions. Evaluation of the effects of cyclic loading are performed using pre-cracked tensile test specimens (PFT) and bulk specimens by Moiré Interferometry. Development of finite element and simple micromechanical models for predictions of the observed behavior also presented. It is observed that hysteretic load-displacement loops arise as the primary characteristic of the behavior, although gross-slip behavior is seen under certain circumstances.

The results of this study conclude that the single most important parameter responsible for the observed behavior, whether hysteretic or gross residual displacement behavior, is contact point density. The results show a direct link between the behavior observed and the microstructural features that are active, mainly elastic bridges and the conversion the

elastic to sliding bridges that dissipate frictional energy. It is also concluded that a distribution of residual stresses and grain stiffness is required to correlate with the observed behaviors. Evidence of both, large and small scale debris is also found after cyclic loading. Large scale debris is primarily found in small grain size aluminas, whereas small scale debris is observed in high cyclic fatigue specimens. Small scale debris is primarily the result of mechanical wear.

1. Objectives: No change from proposal

2. Basic Research Issues

- Determination of crack growth toughening mechanisms in structural ceramics at all temperature conditions of relevance.
- Relate operative toughening mechanisms to the microstructure in a universal manner.
- Measurement methods of specimen displacements at high temperatures were developed and adapted to the demands of the present challenge. Presently, moiré interferometry will be used for DCB characterization in all temperature ranges studied.
- Development of a model descriptive of the physical principles.

3. Approach

- PFT methods will serve as the primary tool for the determination of the link between the microstructure and the behavior.
- Use optical methods for high temperature displacement measurements (Moiré Interferometry).

- Micromechanical modeling is utilized to examine the role of the microstructure on the observed cyclic behavior.
- A novel micromechanical approach to FEM-based model will incorporate the basic elements of the microstructure for a universal microstructural design method.

4. *Significant Results*

Fracture Process Zone Characterization: Cyclic Loading Results (U of H)

The single most prominent feature of the load displacement behavior in a PFT specimen under cyclic loading is the formation of a hysteresis loop. A typical set of load-displacement curves is shown in Figure 1. The maximum test load was progressively increased for each cycle. Although the data curves would be normally displaced by the residual amount of the previous cycle, all the curves are shown at the origin. The data is shown this way to validate the assumption that no gross wake zone damage is occurring during the initial stages of the test, as indicated by the unchanged specimen compliance. A linear-elastic behavior is observed as the specimen is loaded to 0.22kg which is then unloaded. Following the behavior relating to the role of contact density we may conclude that the majority of the contact points in this portion of the wake zone act as elastic contacts throughout the load range of cycle 1. This is a reasonable assumption, as the smallest COD characterizes this part of the wake zone, which is immediately behind the crack tip. One would expect to find the greatest population bridging grains in this region.

With the increase of the maximum load in cycles 2 through 4 in Figure 1, a hysteresis loop develops. This is an indication that some of the elastic points present at lower load levels begin to slide, thus converting to slip contact points. The tangential shear stress

acting on these contact points has increased sufficiently to overcome the local critical shear stress, which results in the increasing compliance observed.

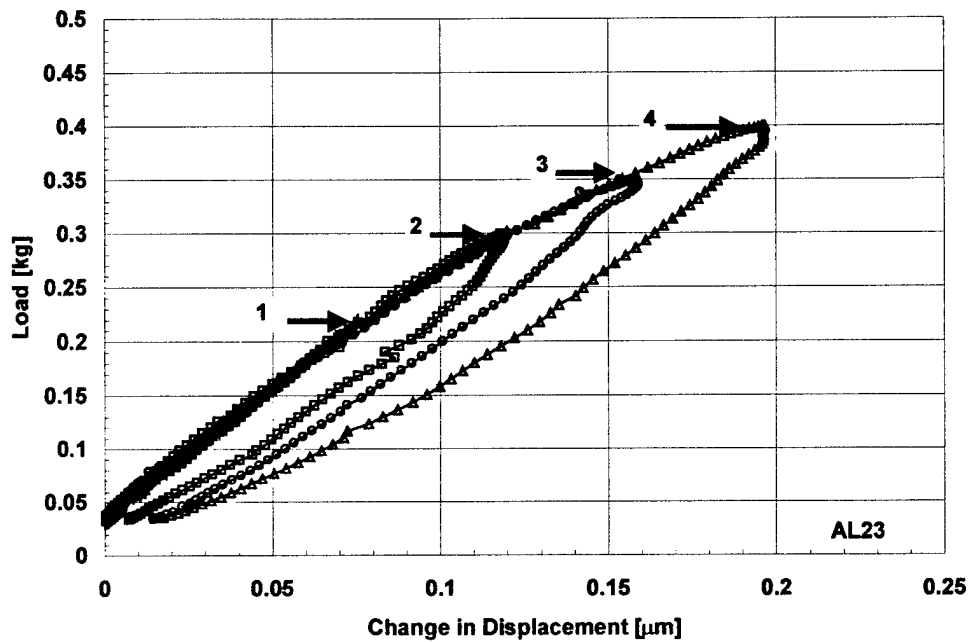


Figure 1 Effect of progressive loading in the evolution on a nearly closed hysteresis loops in alumina

Because the nature of the loading and unloading event includes the dissipation of energy by frictional sliding, it is observed that the hysteresis loops do not fully close when unloaded. The nature of the PFT test, where only tension loading is allowed due to the nature of the geometry of the lower loading groove dictates that the energy available to return the loop to a nearly closed state comes solely from the elastic energy stored in the system.

A distinctively different behavior, namely open loop behavior, was observed for all of the larger COD PFT specimens, regardless of microstructure. A typical open loop

behavior is presented in Figure 2. In this test, the FPT specimen is initially loaded to 0.15 Kg, where nearly linear elastic behavior is observed. Further cycles at larger maximum loads, result in a hysteresis loop characterized by a sharp transition point and large residual displacement. This behavior is associated with the formation of a new bridging system and generation of large-scale debris.

The case presented here is different from case presented before, in that any subsequent loading cycle that is applied to this specimen results in a distinctively open loop behavior. The formation of open loop behavior is the result of gross slip, and the continuous formation of new bridging systems with subsequent loading. At this load, a mass conversion of stick to slip contact points occurs leading to the gross slip behavior observed in cycles 2, and 3. Continuation of this test at the level of loading that causes gross slip would have resulted in certain failure of the specimen in the cycles immediately following the ones shown. Instead of continuing this experiment, the maximum loading is reduced back to the initial load of 0.15 Kg, to assess the condition of the wake zone. It is observed that a nearly closed hysteresis loop is formed once again, but closer examination of the loop, by comparison to the initial test cycle reveals degradation of the wake zone, as indicated by the increased specimen compliance.

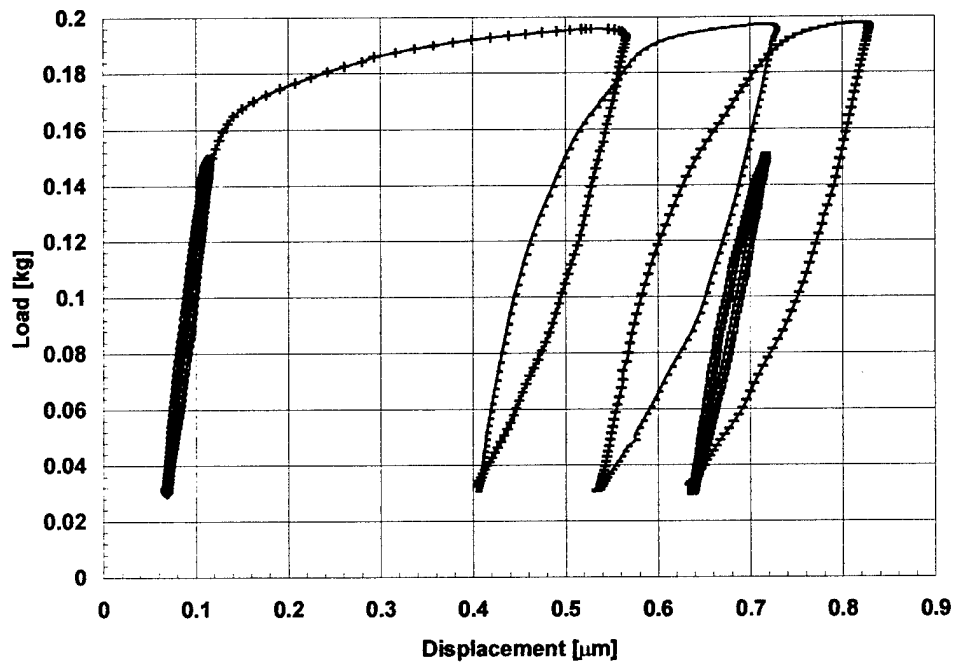


Figure 2 Effect of increased loading and resulting open loop behavior on a PFT 3 AL23 specimen

The typical effects of long term, or high, cyclic loading are shown in Figure 3. Cycles 1, 100, 1000 and 4000 are presented for the same PFT. Here, it is observed that as load cycling progresses the frictional sliding force (force that resists the movement of slip contacts) is reduced. This may result from a combination of two different mechanisms. Firstly, the frictional coefficient between contact points may be reduced due to some smoothing of the interface. Secondly, removal of interface material, as a result of wear, would make the normal forces on the bridging grains decrease. Both of these mechanisms acting alone or simultaneously could be responsible for the observed behavior. Also, it is of note that the load which determines the onset of sliding, i.e. where the initial loading compliance begins to increase, reduces with increasing cycle number. The onset of sliding

is shown for both cycles 1 and 4000. Interestingly, the initial compliance remains constant, which indicates that the number of contact points does not change throughout this test.

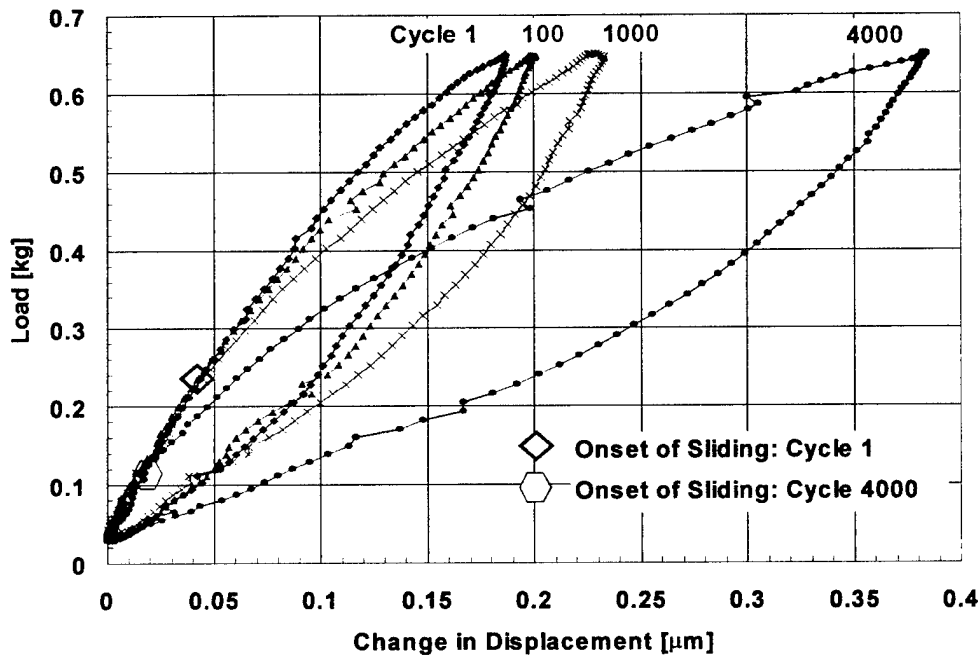


Figure 3 Effects of Long Term Cyclic Loading

Fracture Process Zone Characterization at Elevated Temperatures: Cyclic Loading Experiments Set-up (U of H)

The effects of elevated temperature testing are presented in Figure 4. Initially, at room temperature, linear elastic behavior is observed, where minimal sliding occurs. However, as the temperature is increased to 600°C , while maintaining the load constant, the formation of a hysteresis is observed. It is believed that this is due to the relaxation of the normal (clamping) forces on the bridging grains resulting from the reduction of the thermal elastic anisotropic effects present at room temperature. This results in lower

threshold loads for the sliding of contact points. Upon additional increase of temperature to 800°C further relaxation of the normal forces is observed, resulting in the ratcheting behavior previously observed at room temperature.

As in the previous section, the comparison of the initial and final loading curves in this experiment, show evidence of FPZ degradation.

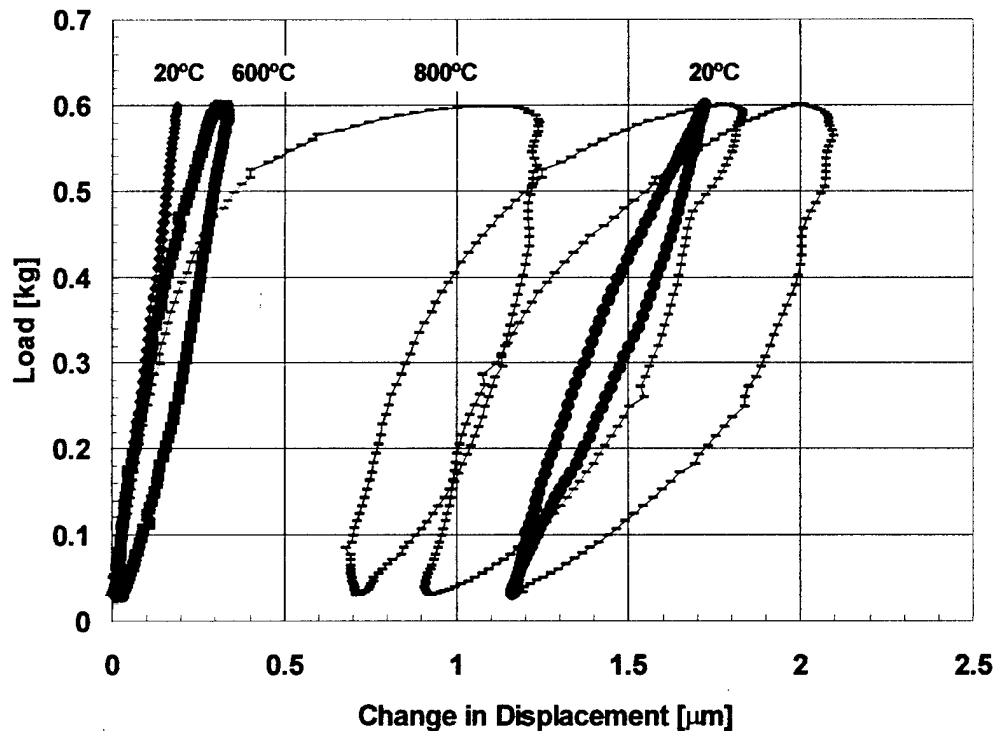


Figure 4 Effects of Temperature on PFT Behavior

A comparison of the behavior of two alumina ceramics at elevated temperature is shown in Figure 5. This comparison is essential in the evaluation of the microstructural effects, since these curves represent crack opening displacement and temperature

conditions that are similar. The initial crack opening displacements for both tests is estimated at 825 nm for both cases, where most of the active grains are still active in the wake zone. The curves show that the load-displacement curve for AL23, which was tested at 0.45 Kg maximum load, would have probably failed at a slighter larger maximum load since the compliance at the maximum load point is very large.

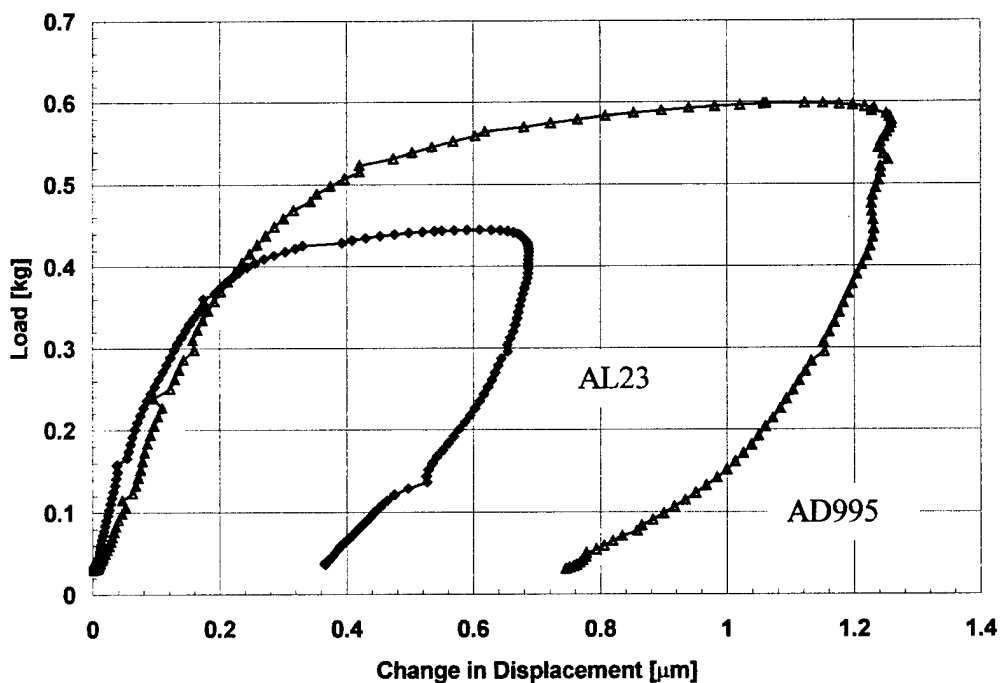


Figure 5 Elevated temperature (800 C) test loops comparing wake zone load capacity of a PFT 2 for two alumina microstructures

The AD995 curve, however, indicates a higher load or bridging capacity as it could be tested to 0.6Kg, with final compliance values that show a potential ability for higher load capacity. Considering that both PFT specimens were produced from temperature interrupted DCB fracture tests, and considering that COD and temperature conditions are similar, it could then be concluded that the differences observed in the load-displacement curves between the two alumina microstructures is strictly the result of active grain bridge

systems. Since the initial crack opening displacements associated with these tests show that the small grain size range grouping (0-6 microns) for AL995 are active in the wake zone, then the additional load or bridging capacity for AD995 can, once again, be attributed to the ability of small size grains to provide load path between crack faces.

Micromechanical Modeling at U of H

An attempt to model the PFT by use of simplified modeling indicated very early in the program that the system, as modeled, would never have enough stored elastic energy to produce hysteretic loop behavior. It was clear from the initial results, that some distribution of elastic and frictional contributions was needed to adequately model cyclic loading behavior.

The incremental piecewise linear model is proposed as a representation of a set of wake zone elements groups that contribute to the total bridging event. The model, shown in Figure 6, represents the wake zone as a distribution of elements that have different elastic and slip characteristics. A distribution means that grain-bridging elements will have different degrees of contribution, i.e., some will move more easily than others will. The remainder of the grain bridges that do not contribute in slip or frictional dissipation, are modeled as the large spring.

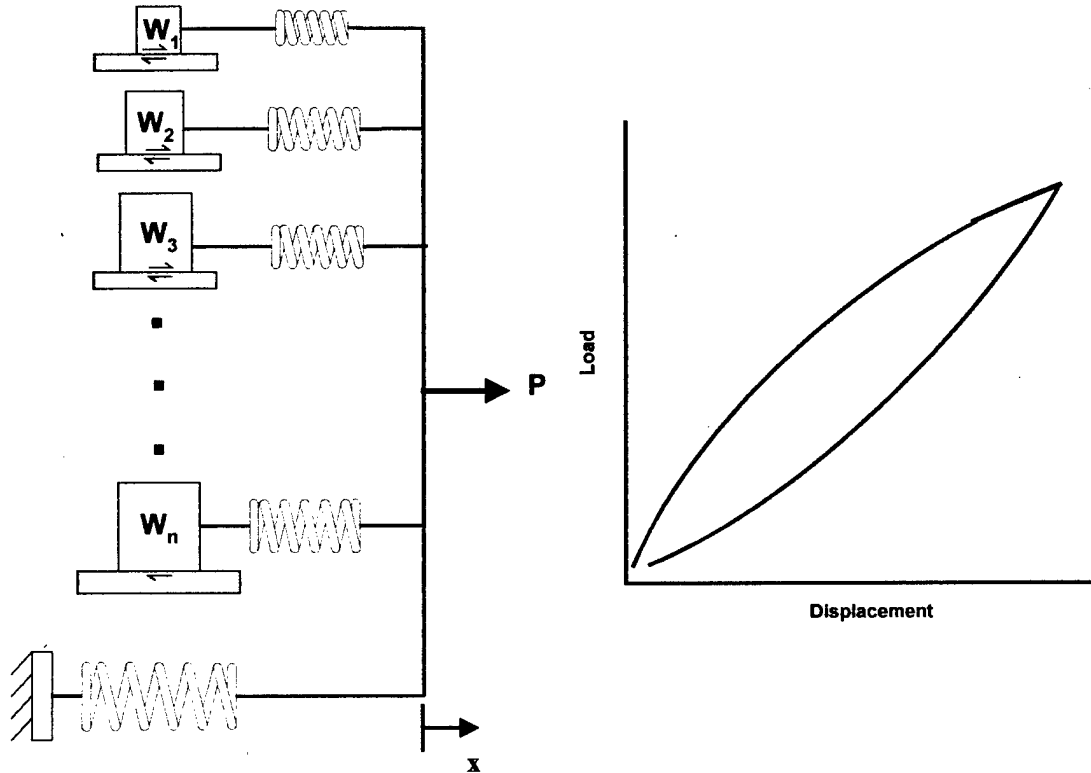


Figure 6 Schematic representation of the piecewise linear model and resultant load-displacement record

Nearly closed-loop hysteretic behavior has been qualitatively described in the previous sections as the case where a high contact point density, dominated by elastic contact points is present in the wake zone. Shown in Figure 7, is a typical nearly-closed hysteresis loop corresponding to a AD995 PFT 1. Unlike the results of simplified modeling, a correlation to these test conditions was clearly obtained by use of the piece-wise incremental model.

To achieve this correlation, the modeling was subjected to the restrictions of a maximum initial compliance of $0.2 \mu\text{m}/\text{Kg}$. A statistical distribution of normal forces and elastic contributors, as represented by the mass of the blocks and springs were obtained. These distributions were subject to the conditions that the elastic contributions could not

exceed $52 \text{ N}/\mu\text{m}$, which is equivalent to the initial stiffness of the system evaluated here. The individual elastic stiffnesses which comprised the distribution ranged between 2.3 and $5.1 \text{ N}/\mu\text{m}$. An additional stiffness element of $5 \text{ N}/\mu\text{m}$ is added, which represent the remainder of elastic contributions that stay elastic throughout the simulation, i.e., do not contribute with sliding effects.

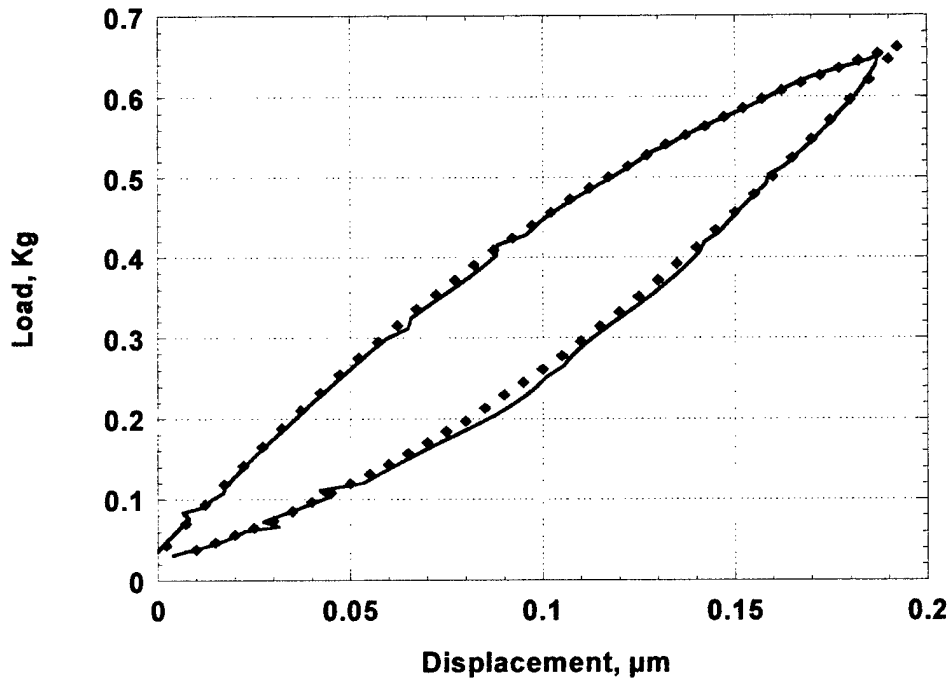


Figure 7 Room temperature incremental piecewise model correlation

The incremental piecewise modeling also provided excellent elevated temperature correlation. An example of the correlation of Thermal Expansion Anisotropic (TEA) effects is shown in Figure 8. In here, back-to-back tests are performed on the same specimen at similar test conditions. A room temperature test is first performed, which is

then followed by an elevated temperature test at 600C. The test results are shown by the solid lines.

A successful correlation was obtained by first obtaining a correlation at room temperature. A correlation is then obtained at 600 C, by modifying the residual stress distribution array to reduce the normal forces by 42%, which is in excellent agreement with residual stress reduction calculations available in the literature.

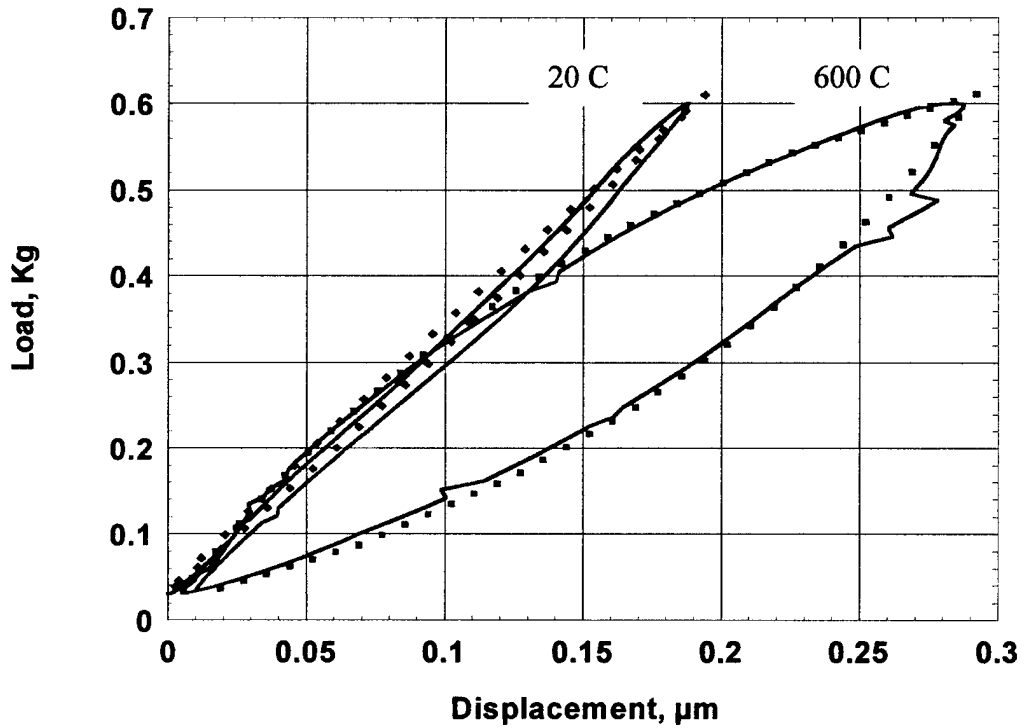


Figure 8 Correlation of thermal expansion anisotropic effects

An important finding of the correlation exercises is that there are microstructural events that can not be accurately modeled. These features include observations that tests performed on specimen of larger COD and that are associated with higher loads, causes the effective bridging lengths of smaller grains to be exceeded, causing dislodging and repositioning of these particles in the wake zone. The particles then interfere in the motion of the wake, causing artificial crack opening displacements, which are later reduced as the result of pulverization or accommodation of debris under subsequent cycles of loading. It is important to recognize that the scale of residual displacement falls in the order of this particle size, considering the cumulative residual displacement for the entire test sequence. An example of large-scale debris is shown in Figure 9.



Figure 9 Fracture surface topography showing large scale debris in AD995

Micromechanic Modeling (U of W)

The fracture process zone (FPZ) of two polycrystalline alumina fracture specimens were analyzed by a hybrid experimental-numerical procedure involving a phase-shifting moiré interferometry and a newly developed moiré grating for room and high temperature testings, respectively. The resultant displacement field provided the input to a finite

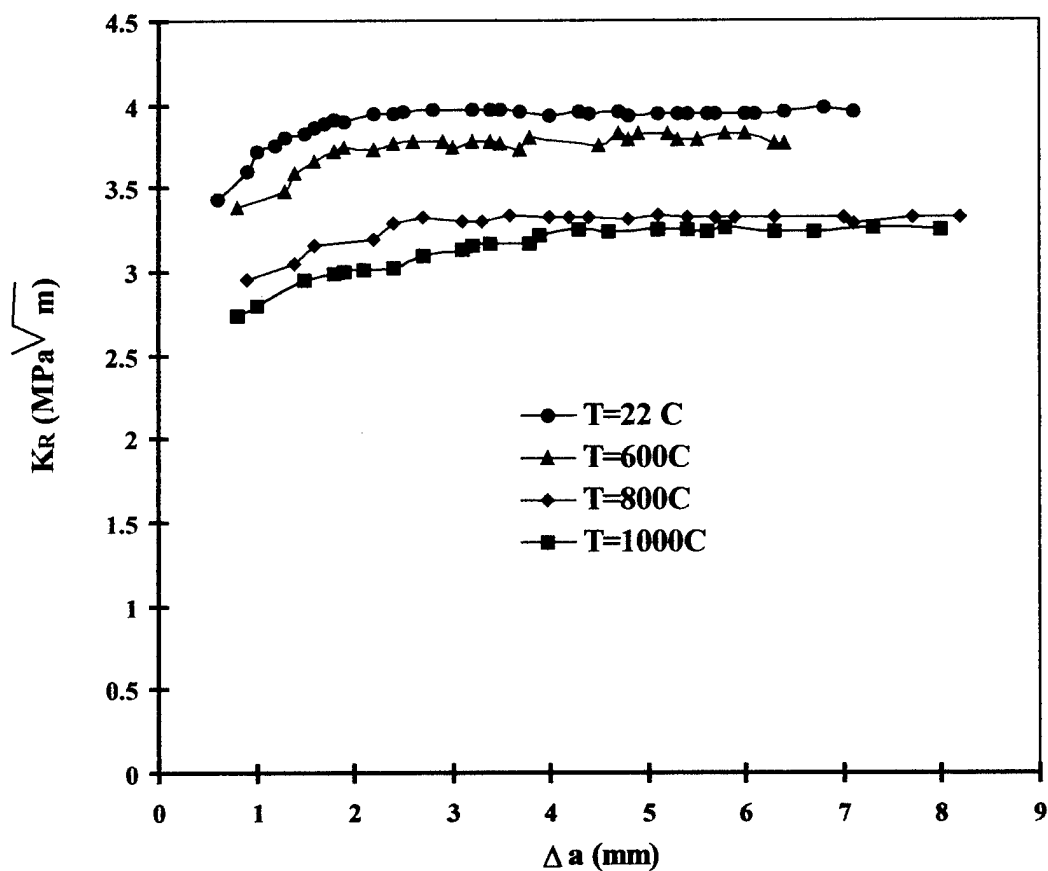


Figure 10. K_R curves for AL-23 alumina.

element model of a wedge-loaded, double cantilever beam (WL-DCB) specimen geometry of two microstructures of commercial alumina. The crack closing stress in the FPZ decreased precipitously with increasing crack opening displacement. The change in the

fracture resistance, i.e. K_R -curves, with increasing temperature for the 99.7% commercial alumina (AL23) are shown in Figure 10.

These results are consistent with earlier directly-measured K_R -curves, reported in this program, where thermoelastic residual stresses dominate below 700C, as characterized by lower plateau values with increased temperature. At higher temperature, the effect of reduced viscosity of the glassy interface is indicated by both reduced plateau levels and K_R -curve flattening. The fracture energy dissipated in the FPZ is about 95 percent of the energy released thus showing that the FPZ is the major energy dissipation mechanism in the brittle alumina.

The results of a second generation model of the FPZ have been investigated in more detail. The experimental and computed bridging stress versus applied displacements for a low cycle fatigue test were found to be in agreement. An analysis of the individual bridging grains in this second generation model has now been performed. The purpose of this analysis was to provide insight into the details of crack bridging.

The FE model did not include any explicit forms of degradation such as a decrease in the coefficient of friction due to wear yet it modeled the experimental results satisfactorily. An analysis of the individual crack bridges showed increased pullout of the grain at unloading after each successive cycle as seen in Figure 11. This "residual pullout" was responsible for the degradation effect in the FE model. It is unclear at this point whether this "residual pullout" can fully explain the degradation of the grain bridges at low-cycle tension-tension, but it remains a possibility.

During the course of this analysis, several limitations were identified in the second generation model. The second generation model was composed of eleven individual models each pertaining to a different grain size. Load control of this model was not possible due to the different load carrying capacities of each model. In addition, the

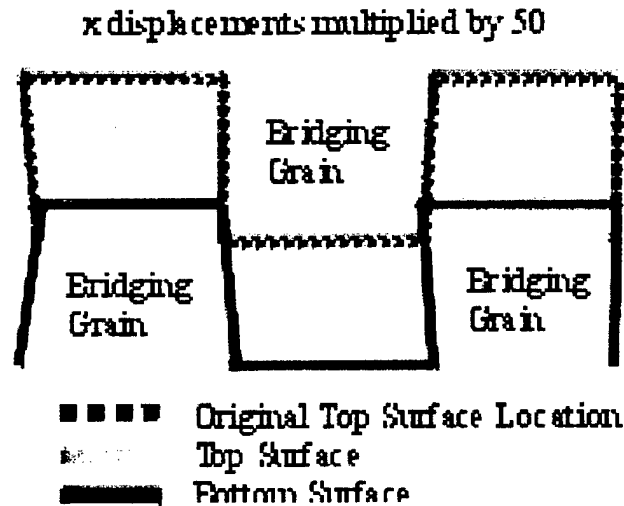


Figure 11 Residual Pullout

dimensions of the largest model were 6.625 times larger than the smallest model due to the restriction of having the same number of elements in each model. While this effect was neutralized in the cross-sectional plane by dividing the force by the cross-sectional area, no such solution was possible for the dimension parallel to the load line. This results in a smaller “net applied displacement” at the crack interface in the larger grains.

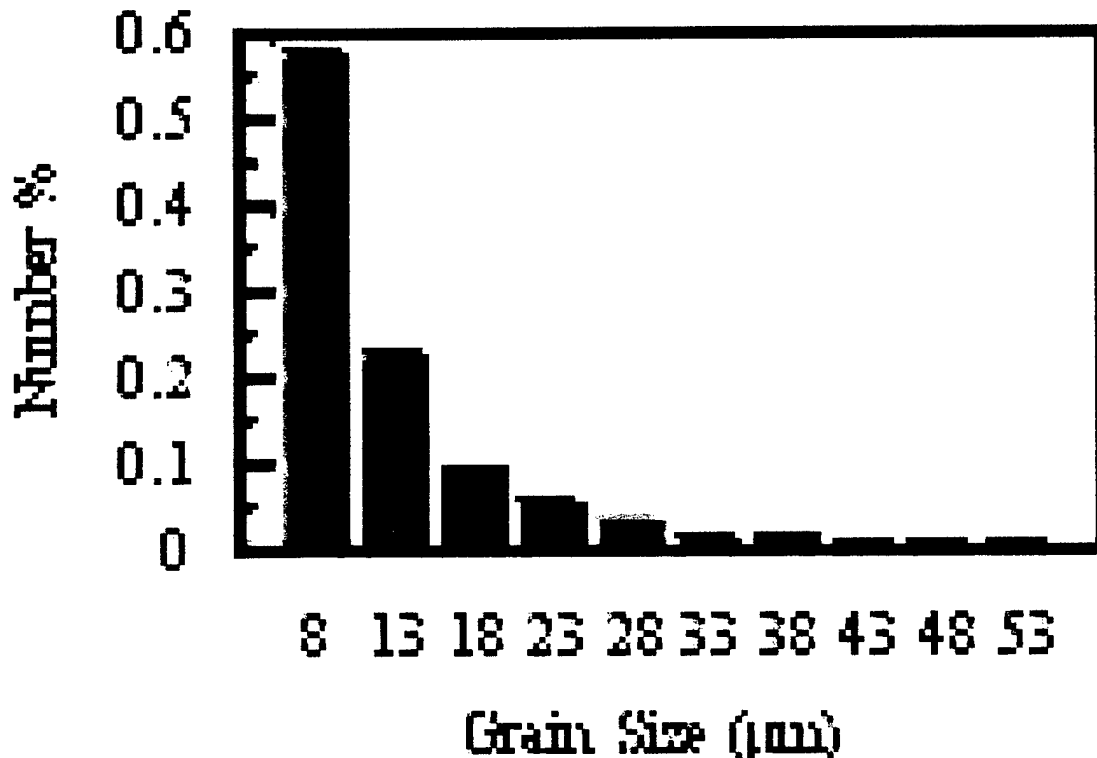


Figure 12 Number Percent of Grain Size Distribution

When the interfacial stresses between bridging grains were analyzed, the interfacial stresses in the larger grain size model were much larger than those in the smaller due to the larger strain mismatch. In the “real” material, the average interfacial stresses are smaller because of the large probability that a large grain will be interacting with a small grain. This becomes more obvious when the grain size distribution is plotted in terms of numbers of grain instead of grain area as seen in Figure 12. As a result of these and other minor issues, it was determined a third generation model should be developed. This third generation model will be a “unified” model where all the grains are modeled in one FE mesh. In addition, attempts will be made to model a more complicated (and real) crack path.

A third generation hybrid experimental-numerical procedure was used to analyze the results from low cycle fatigue tests on AD998 alumina at room ($\sim 25^{\circ}\text{C}$), 600°C and 800°C temperatures. A double cantilever beam (DCB) specimen was pin loaded and driven by a piezoelectric transducer. Unfortunately, the pin gradually “stuck” in the specimen after ~ 50 cycles at room temperature and after only 1 or 2 cycles at higher temperatures. This was not recognized until after tests were performed and modeling began. During the subsequent cycles, the minimum load observed by the specimen gradually increased to the maximum load. Because of this, relevant data was only available during the first two or three cycles of the fatigue test during which $0 < R < 0.1$. Phase shifting moiré interferometry was performed on the specimens at various steps in the loading and unloading of the specimen.

The moiré data was used in a subsequent finite element model to determine the crack closure stress (CCS) caused by bridging grains in the fracture process zone (FPZ). The DCB specimen was modeled exactly as shown in Figure 14. The model consisted of 50 micron square elements near the crack path and 100 micron square elements farther from the crack. The displacement information from the phase-shifted moiré was used to generate a crack profile which was subsequently used as boundary conditions on the crack faces. At the location of the pin loading, displacement data was used as boundary conditions in the horizontal direction and load cell data was used as a boundary condition in the vertical direction as shown in Figure 14. The resulting reaction force at the crack face was used to calculate the crack closure stresses (CCS). An Environmental Assisted Scanning Electron Microscope (ESEM) was used to observe crack bridges as seen in Figure 15.

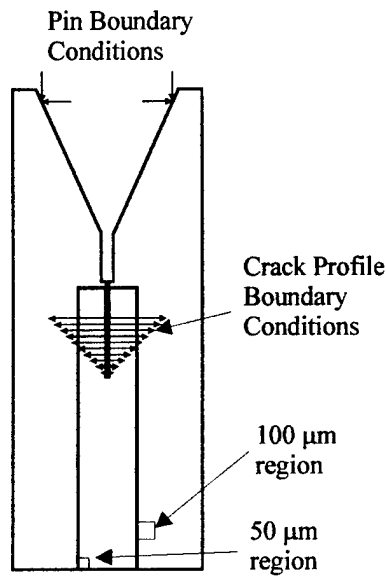


Figure 14. FEA Model

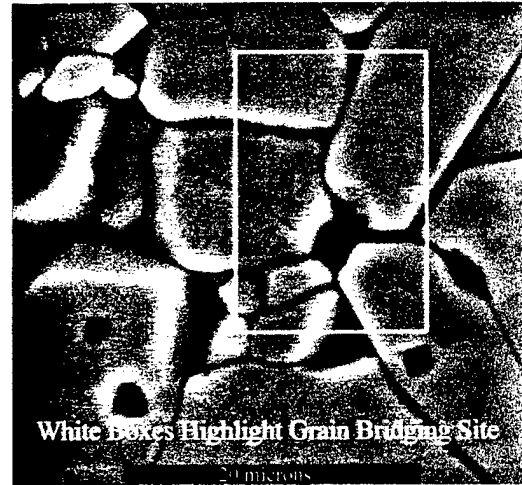


Figure 15 SEM Photo of Grain Bridge

The resulting crack profiles from the moiré data at several loads and unloads at room temperature are shown in Figure 16. The resulting horizontal load at the pin load is indicated in the legend. During unloading of the crack, it appeared that crack bridges provided a “crack closure” effect. As a result, the grain bridges near the crack tip did not return to their original un-cracked location. This artifact remained during subsequent loading and un-loading . The source of “crack closure” is attributed to the re-initiation of contact between grain bridges that were previously separated while loaded at the maximum load. 600°C and 800°C specimens exhibited the same effect. This is shown for the 800°C specimens in Figure 17. The “crack closure” effect and resultant residual opening remained with the pin removed from the specimen indicating that this effect was not due to the pin sticking.

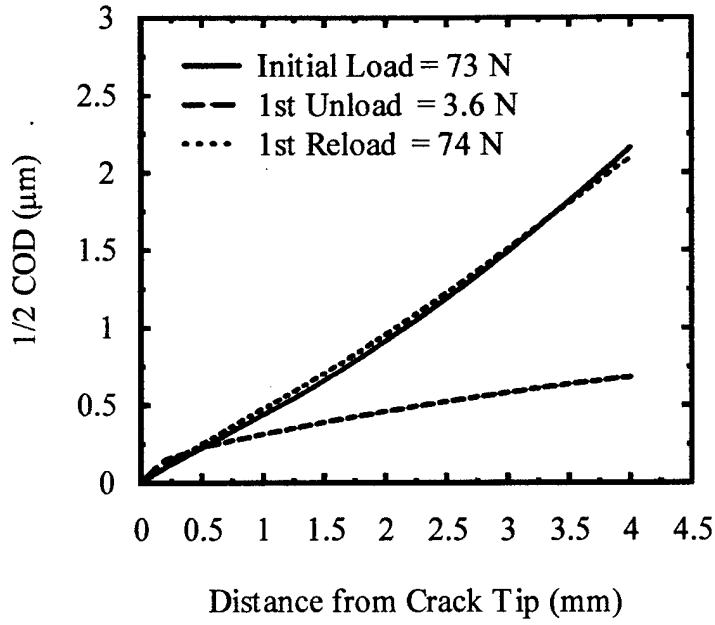


Figure 16 Crack Profiles at Room Temperature

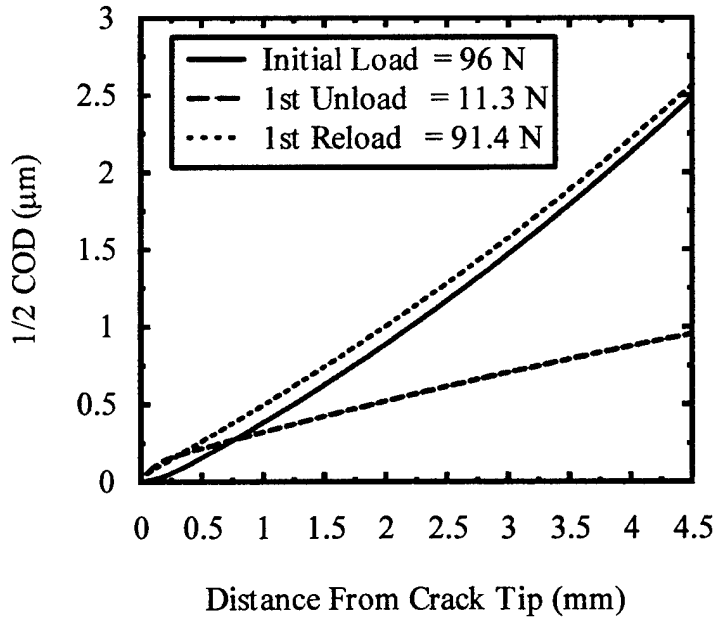


Figure 17 Crack Profiles at 800°C

The crack closure stress for a room temperature test during loading, unloading, and subsequent reloading are shown in Figure 18. During the unloading phase, the CCS stresses become negative as the grain bridges resist returning to their original positions due to frictional contact. This was similarly observed at both 600°C and 800°C. The

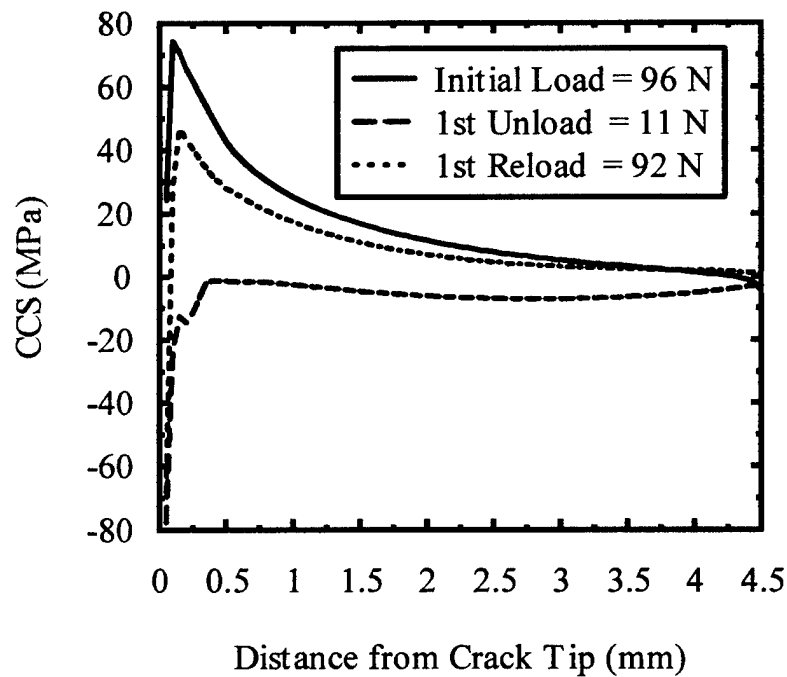


Figure 18. CCS Stresses at Room Temperature

800°C data is shown in Figure 19. Comparison between temperatures shows a decrease in CCS stresses as the temperature increases at peak load while the stresses at unload are similar for all temperatures

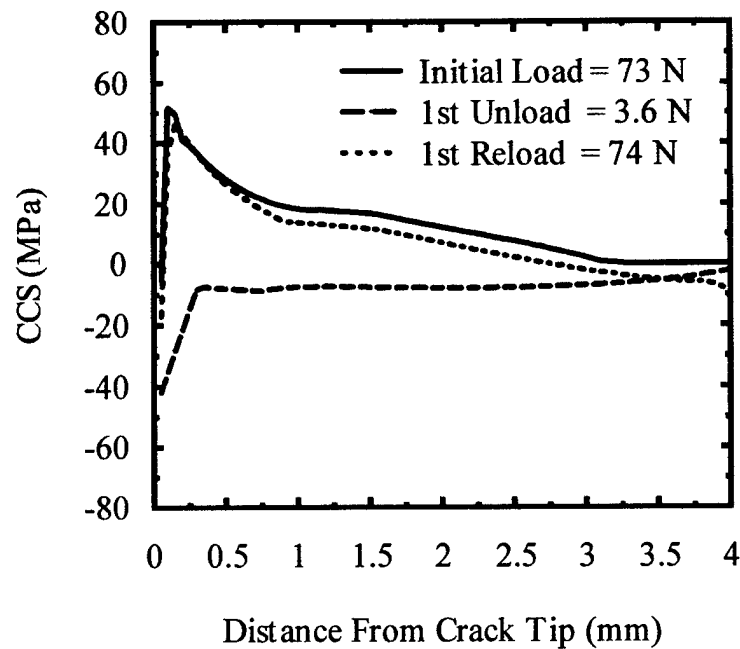


Figure 19 CCS Stresses at 800°C

As a result of this initial analysis, it appears that $R > 0$ fatigue does not result in a full range of grain sliding. A “crack closure” effect reduces the amount of grain sliding at bridging sites. This reduction in grain sliding reduces the amount of wear possible during $R > 0$ fatigue. This may be extended to other materials such as self-reinforced silicon nitride with beta phase grains which exhibits a dependence of crack growth rate on R .

5. *AF Relevance*

- Develop microstructure-based methods for design of improved toughness ceramics.
- Initiate basis for component design methodology for brittle materials.

Acknowledgment/Disclaimer

This work was sponsored by the AFOSR, USAF, under grant F49620-96-1-0451. The views and conclusions contained herein are those of the authors and should not be interpreted as necessarily representing the official policies or endorsements, either expressed or implied, of the Air Force Office of Scientific Research of the U.S. Government.

Publications Generated Through AFOSR Grant No. F49620-93-1-0210.

Refereed Journal Articles

"Grain Boundary Phases and Wake Zone Characterization in Monolithic Alumina," J.C. Hay, K.W. White, *J. Am. Ceram. Soc.*, **78** [4], pp. 1025-1032 (1995)

"The Stiffness of Grain Bridging Elements in a Monolithic Alumina," J.C. Hay, K.W. White, *J. Amer. Ceram. Soc.*, **80** [5], pp. 1293-97, (1997)

"Fracture Process Zone Modeling of Monolithic Al₂O₃," Z.K. Guo, J.C. Hay, K.W. White and A.S. Kobayashi, *Engineering Fracture Mechanics*, **63**, pp. 115-129 (1999)

"Process Zone of Polycrystalline Alumina," D.K. Tran, A.S. Kobayashi and K.W. White, *Experimental Mechanics*, **39** [1], pp. 20-24 (1999)

"Fatigue Degradation of Grain Bridging Elements in a Monolithic Alumina," R.Geraghty, J.C. Hay, K.W. White, *Acta Metallurgica et Materialia*, **47** [4], pp. 1345-1353 (1999)

"Fracture Process Zone Modeling of Monolithic Al₂O₃," Z. K. Guo, J. C. Hay, K. W. White and A. S. Kobayashi, *Engineering Fracture Mechanics*, **63**, 115-129 (1999)

"Modeling of Grain Pullout Forces in Polycrystalline Alumina," M.T. Kokaly, D.K. Tran, A.S. Kobayashi, X. Dai, K. Patel and K.W. White, *Material Science and Engineering*, **A 285**, pp. 151-157 (2000)

"Bridging Stress Relation from a Combined Evaluation of the R-curve and Post-fracture Tensile Tests," T. Fett, D. Munz, D. X. Dai, and K. W. White, Accepted in: *Int. J. of Fracture*, (2000)

"Crack Growth in Alumina at High Temperature," D.K. Tran, A.S. Kobayashi and K.W. White, to be published in *Engineering Fracture Mechanics*.

"Characterization of Microstructure-Mechanical Behavior Relationships of Crack Wake Zone Bridging Elements in Monolithic Ceramics Under Cyclic Loading" L. Olasz, C. R. Ortiz-Longo, and K.W. White, To be submitted to: *Journal of the American Ceramic Society*.

Conference Papers

"Experimental Techniques in Dynamic Fracture," A.S. Kobayashi, *Proceedings of International Symposium on Advanced Technology in Experimental Mechanics*, JSME, pp 7-11 (1995)

"Microstructural Characterization of an *In Situ* Grown Si₃N₄ Whisker-Reinforced BAS Glass-Ceramic Matrix Composite," F. Yu, C. Ortiz-Longo and K. W. White, *Ceram Trans.*, **74**, pp. 203-14 (1996).

"Wake Process Zone Characterization in a Structural Ceramic," J.C. Hay and K.W. White, *Fracture Mechanics of Ceramics*, **11**, pp. 75-94, eds. R.C. Bradt, et al., Plenum Publishing Co., (1996)

"Process Zone Modelling of Polycrystalline Alumina," D.K. Tran, C.-T. Yu, J.C. Hay, K. White and A.S. Kobayashi, *Fracture Mechanics of Ceramics*, **11**, pp. 29-38, eds. R.C. Bradt, et al., Plenum Publishing Co., (1996)

"Process Zone of Polycrystalline Alumina," D.K. Tran, A.S. Kobayashi and K. W. White, *Advanced Technology in Experimental Mechanics '97*, JSME, pp. 245-248, (1997)

"Fracture Process Zone of Polycrystalline Alumina," D.K. Tran, A.S. Kobayashi and K. W. White, *Composites and Functionally Graded Materials*, ASME MD-Vol. **80**, pp 361-364, eds. T.S. Srivatsan et al, (1997)

"Crack Growth in Alumina at High Temperature," D.K. Tran, A.S. Kobayashi and K. W. White, *Advanced Technology in Experimental Mechanics'99*, Japan Society of Mechanical Engineers, No. 99-204, pp 527-532. , July 1999

"Micro-Mechanical Modeling of the Fracture Process Zone of Alumina," M. Kokaly, D.K. Tran, A.S. Kobayashi and K.W. White, *Progress in Experimental and Computational Mechanics in Engineering and Material Behavior*, pp. 4-12, eds. D. Zhu, M. Kikuchi, Y. Shen and M. Geni, Northwestern Polytechnical University, China, Sept. 1999

"Fracture Process Zone of alumina WL-DCB Specimen Under Cyclic Loading," M.T. Kokaly, D.K. Tran, A.S. Kobayashi and K.W. White, *Proceedings of the IX International Congress on Experimental Mechanics*, pp. 294-297, Society For Experimental Mechanics, June, 2000